Send Orders for Reprints to reprints@benthamscience.net

Recent Patents on Engineering, XXXX, *XXX*, e18722121286139

REVIEW ARTICLE

A Decade of Prostate Intervention Robots: Systematic Review

Weixi Zhang[1,2,3,*] and Jiaxing Yu[2]

[1]*Key Laboratory of Advanced Processing Technology and Intelligent Manufacturing, Heilongjiang Province, Harbin University of Science and Technology, Harbin, Heilongjiang, 150080, China;* [2]*Harbin University of Science and Technology, Harbin, Heilongjiang, 150080, China;* [3]*Postdoctoral Research Center of Instrument Science and Technology, Harbin University of Science and Technology, Heilongjiang, 150080, China*

ARTICLE HISTORY

Received: April 18, 2024
Revised: June 06, 2024
Accepted: June 11, 2024

DOI:
10.2174/0118722121286139240827074802

Abstract: The image-guided prostate intervention robot can assist surgeons in performing minimally invasive intervention procedures. It has the advantage of overcoming the disadvantages of a traditional surgeon's hand tremor and dependence on the need for an experienced surgeon, improving the intervention precision, and reducing the hazards caused by normal soft tissues due to surgical precision errors compared to traditional intervention procedures. In the design of prostate intervention robots, structural design, materials, actuators, and compatibility issues should be considered. Based on the above considerations, a representative literature of the last decade was selected for review.

Patents and articles on image-guided prostate intervention robots published in the last 10 years (2013-2023)were searched in several electronic databases, focusing on keywords (structural design, puncture accuracy, image compatibility, actuator) for screening.

We retrieved a total of 26 prostate intervention robots guided by different images, classified them by US, MRI, MRI-US and CT, selected representative robots guided by different image modalities for review and tabulated them for comparison, and finally boldly predicted that the future direction will be prostate robots guided by MRI-US images.

Image-guided prostate intervention robots can improve the deficiencies of conventional intervention procedures. In the future how to improve the intervention accuracy will be the primary problem of all intervention robots, through structural design, materials, actuators, and image compatibility issues have been improved.

Keywords: Prostate intervention robots, puncture accuracy, image guidance and compatible, actuator, material.

1. INTRODUCTION

In recent years, prostate cancer has become an increasing concern for men. Globally, approximately 1.41 million cases of prostate cancer are diagnosed each year, and 380,000 of them die from the disease [1, 2]. Treatment options for prostate cancer include radical resection, external irradiation, high-intensity focused ultrasound, and brachytherapy. Of these, BT(BrachyTherapy) has become a major treatment option [3-8]. BT offers many advantages, including minimal trauma, short recovery time, and few side effects. In addition, it does not cause thermal changes in tissues or damage healthy tissues.

BT is usually performed as an intervention procedure using a TP (TransPerineal) or TR (TransRectal) approach [9, 10]. TR ultrasound is a widely used method in most prostate interventions due to its real-time imaging and cost-effectiveness [11]. However, ultrasound-guided prostate intervention robots still face many challenges. For example, the shape of the prostate and surrounding soft tissues can affect the accuracy of the puncture needle during the procedure, leading to needle flexion and glandular edema. In addition, most puncture needles are limited by the guidance mechanism, which severely restricts their flexibility. Although US (Ultrasound Systems) provide real-time imaging, they also have a high rate of false negatives. The use of MRI (Magnetic Resonance Imaging) instead of US can significantly improve imaging quality and puncture accuracy. However, MRI as an image-guided tool can have several disadvantages, such

* Address correspondence to this author at the Key Laboratory of Advanced Processing Technology and Intelligent Manufacturing, Heilongjiang Province, Harbin University of Science and Technology, Harbin, Heilongjiang, 150080, China; E-mail: zwx_9552@163.com

as long consumption time, limited spatial resolution, high cost and limitations in materials, actuators and transducers. In addition, to avoid image distortion caused by strong magnetic fields, some CT (Computed Tomography)-guided punctures have been used in recent years and MRI and ultrasound image alignment methods have been used to achieve higher accuracy [12]. The integration of medical imaging techniques with medical devices is crucial, and good fusion techniques can improve the accuracy of the puncture mechanism [13].

The emergence of prostate intervention robots has the potential to address the limitations of traditional surgery, such as a lack of experience on the part of the doctor, hand tremors due to physiological factors, radiation damage caused by radioactive particles to the doctor, and easy deflection due to improper hand-eye coordination during needle insertion. Therefore, automated prostate intervention robots can often mitigate these deficiencies. The workflow of a prostate intervention robot varies depending on different materials, principles, and scenarios. For instance, different image acquisition methods and DOF (degree-of-freedom) lead to varying levels of flexibility, which in turn affects the functional flow of a prostate intervention robot [14]. As such, it is necessary to classify and summarize the various types of prostate intervention robots based on these differences.

Currently, prostate BT robots still face significant challenges, especially in terms of how to improve the precision of intervention procedures and reduce damage to normal soft tissues. In recent years, with the rapid development of intervention surgical robots, more BT robots have been designed with greater flexibility and applicability. The flexibility of the robots depends on their structural design. For example, Zhang *et al.* proposed a 6DOF articulated particle implantation robot [15], which uses RRT (Rapidly-exploring Random Trees) positioning combined with end-rotation vibration injection to improve puncture accuracy. Fischer *et al.* proposed an MRI-guided prostate surgery robot [16] that allows horizontal and vertical adjustment as well as angular rotation for a wide range of positional and postural adjustments. Kim *et al.* [17] proposed a 2DOF needle driver that uses splines and synchronous toothed belt coordination to achieve translational and rotational modes. Liang *et al.* proposed a prostate biopsy robot guided by MRI, equipped with two actuators in the working plane and one in the rotating plane. The aim is to achieve horizontal, vertical, and rotating functions of the needle [18]. Jiang *et al.* introduced a 3DOF parallel robot with RCM (Remote Motion Center). Through experiments on 20 hunting dogs of different sizes, the final positioning error was approximately 5 mm [19]. In order to address the challenging problem of prostate intervention surgery in confined spaces, Duan *et al.* developed a continuous robot driven by line and constructed a prototype using 3D printing technology. Experimental results demonstrated that the positioning error was less than 2.5 mm [20].

In this paper, we review typical linear brachytherapy robots developed in the last decade based on their structural design, puncture accuracy, material selection, and compatibility with image guidance. Section 2 describes prostate BT robots guided by different imaging systems, and Section 3 describes the compatibility of the puncture robot with image-guided systems and intervention techniques. Our review discussion is presented in Section 4, and the conclusions of this paper are provided in Section 5.

2. PROSTATE INTERVENTION ROBOTS GUIDED BY DIFFERENT IMAGES

2.1. Ultrasound-guided Prostate Intervention Robots

The novel 7DOF robot is proposed by Long for perineal puncture intervention. The robot consists of a needle positioning module and a needle insertion module [21]. The needle positioning module mainly consists of two pairs of translational guides, while the needle insertion module moves linearly *via* ball screws. The needle can also be manually rotated to implant radioactive seeds. Experimental data confirm that the robot has high puncture accuracy, reaching phantom targets with a median accuracy of 2.73 mm and 5.46mm, respectively. However, the mechanism is not bilaterally symmetric in weight and the prostate may be punctured lower in one direction due to the effect of gravity on curvature. C. Vaida *et al.* proposed an intervention soft tissue mechanism with a parallel structure [22]. This mechanism is bulky and has a cantilevered form with 3DOF X, Y, Z. The puncture mechanism incorporates a guide plate and is capable of adjusting the needle angle itself. Although this mechanism is suitable for more applications, it is less rigid, less flexible, uses a parallel mechanism with high difficulty, and has motion singularities. Poquet [23] developed a 6DOF tandem robot cooperative operating system that moves like a human arm. It has FMC (Free Mode Control) and LMC (Locked Mode Control). In the free mode, the ultrasonic probe does not move, while the electromagnetic brake for the wrist, as well as the drive for the shoulder and elbow joints, are in the locked position. The system uses collaborative operations to assist physicians in performing real-time piercings in locked mode. Zhang *et al.* proposed a 6DOF articulated particle implantation robot [15], the cantilever used RRT type as positioning and a parallelogram linkage mechanism was used to improve the stiffness [24]. The robot includes: a positioning module, surgical instrument module, and image navigation module, where the positioning module includes a linear slide that can undergo linear displacement, and the cantilever, linkage, and base form a parallelogram mechanism, the surgical instrument module that is incorporated in this robot is a linear drive mechanism, a rotary drive mechanism, an axial vibration mechanism and a puncture needle composition, where the hollow tube is driven by a servo motor for rotation and linearity. The piezoelectric ceramic component was incorporated inside in order to provide axial high-frequency vibration [25, 26], and the image navigation module is the equivalent of the human eye providing the puncture route through ultrasound paired with the surgical instrument module. The experiment used a new piezoelectric vibration rotary needle feeding device, vibration assisted to achieve high precision puncture, but the current experimental environment is under the pig kidney to obtain data and due to the

cantilever mechanism error, other aspects of the accumulation will also have certain shortcomings. As shown in Fig. (**1A**, **C**) Vaida's *et al.* [27] proposed a transrectal ultrasound puncture biopsy needle intervention mechanism consisting of a 2DOF puncture adjustment module and a 3DOF ultrasound probe adjustment module. The two modules are connected in parallel by a universal joint, and the ultrasound probe module is located below the puncture module. Although the parallel mechanism is more flexible, the positive solution of the parallel robot is more complex and inter-mechanism errors accumulate. Ban *et al.* proposed a 2DOF radioactive particle implantation device [28], which includes: an external needle insertion mechanism, an automatic particle placement mechanism, and an internal needle reciprocating propulsion mechanism. The internal needle sliding table is firmly attached to the ball screw sliding table, the external needle is firmly attached to the internal needle sliding table, and a servo motor drives the sliding table to achieve linear motion. The automatic pellet implantation device works as follows: the spring presses the pellet and guides the inner needle, the outer needle pushes into the pellet toward the lesion point, and the inner needle withdraws to press the pellet in. Lim *et al*., proposes a robot assisted by transrectal ultrasound prostate biopsy robot [29], with a 4DOF adjustment probe and adopted RCM [30-32], with no intraoperative registration [33]. Probe RCM protection can be realized by rotating ξ1 and ξ 2, along the axis of ξ3 to realize linear motion and rotation. The bench test item 2, item 1 imaging test, targeted two *in vitro* tests, and clinical trials of the IRB(Institutional Review Board) approval of 5 patients puncture needles with an accuracy of 1 mm were conducted. Wang *et al.* have developed an ultrasound-guided 8DOF prostate biopsy robot, which integrates a kinematic model to map the unbinding error and improve puncture accuracy. The feasibility of both the kinematic model and the robot has been verified through experiments [34].

A transrectal ultrasound image-guided prostatic puncture robot with the public number CN113367777A was proposed [35]. As shown in Fig. (**1B**), the prostate puncture robot comprises a base 1, a robotic arm module 2, an arc telecentric module 3, a puncture needle clamping module 4, and an ultrasonic probe clamping module 5. Module 2 and module 5 are installed on the base 1. The puncture needle holding module 4 is the end feed mechanism of the prostatic puncture robot, and modules 2, 3 and 4 are connected together successively. The ultrasonic probe clamping module 5 comprises a rotating joint and a moving joint. The ultrasonic probe clamping module 5 is used to realize the feed and rotation motion of the ultrasonic probe and meet the requirements of the ultrasonic probe in puncture guidance. As shown in Fig. (**1C**), GB1331341 demonstrates a 4DOF prostate puncture robot guided by ultrasound [36]. The targeted puncture auxiliary device includes ultrasonic probe 1, probe tilt mechanism 2, Z stepper 3, YZ stepper connector 4, X stepper 5, Y stepper 6, sample bench 7, casters 8, body film fastener 9, and body film 10. The motion mode includes a moving module in the XYZ direction of 3DOF and a probe pitching mechanism 2; when the robot works, it first controls the pitting mechanism 2 to keep the probe 1 level, then adjusts the X stepper 5 and Z stepper 3 to align the probe with the human body, and also the Y stepper 6 to enter the probe into the human body. In order to obtain a clear ultrasonic image, the probe can be pitted, while keeping the probe end fixed, the required movement is compensated by the Y stepper 6 and Z stepper 3. CH113331875B proposed a prostate biopsy and puncture robot based on ultrasonic image guidance [37], the main structure of which is shown in Fig. (**1D**), including angle control mechanism 1, ultrasonic probe fixing mechanism 2, vertical position adjustment mechanism 3, and puncture execution mechanism 4. The ultrasound images in two different planes of the patient's prostate were obtained by the transrectal ultrasound probe, and the motion was carried out by the angle control mechanism, the vertical position adjustment mechanism, and the puncture actuator to accurately control the puncture needle. Patent US8702579B2 [38], as shown in Fig. (**1E**), is a 7DOF prostate puncture robot. The robot can realize two functions of positioning and puncture, positioning its own injection angle through 5DOF, and implementing injection through 2DOF. The mechanism works in both horizontal and vertical space, with a transverse translation of 105mm, a head-to-tail translation of 90mm, and a sagittal and coronal deflection of 30°.

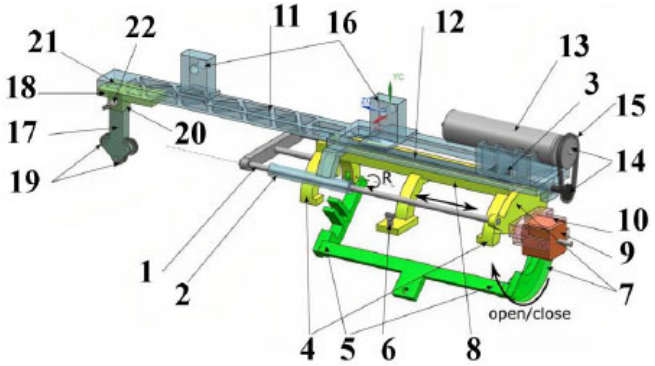

Fig. (1A). The needle insertion module [27]. *(A higher resolution / colour version of this figure is available in the electronic copy of the article).*

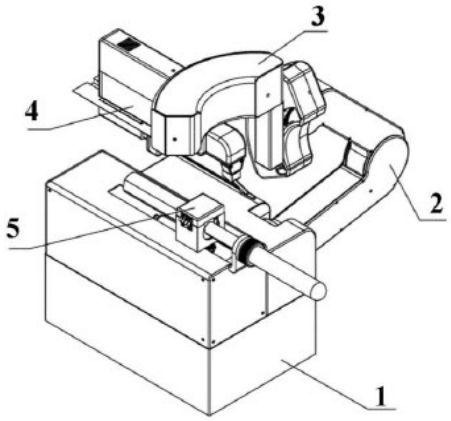

Fig. (1B). The prostate puncture robot(CN113367777A) [35]. *(A higher resolution / colour version of this figure is available in the electronic copy of the article).*

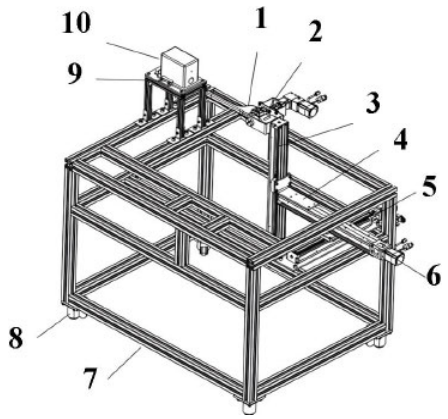

Fig. (1C). The prostate puncture robot(GB1331341) [36]. *(A higher resolution / colour version of this figure is available in the electronic copy of the article).*

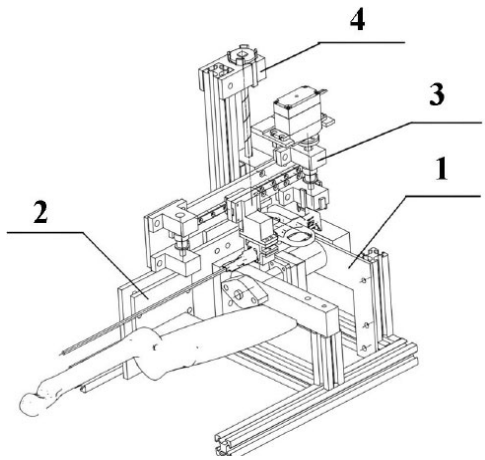

Fig. (1D). The prostate puncture robot(CH113331875B) [37]. *(A higher resolution / colour version of this figure is available in the electronic copy of the article).*

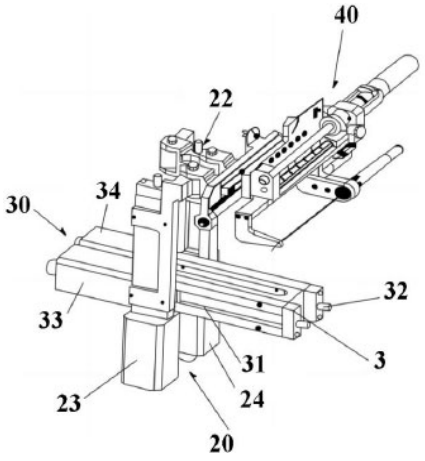

Fig. (1E). The prostate puncture robot(US8702579B2) [38]. Ultrasound-guided prostate intervention robot. *(A higher resolution / colour version of this figure is available in the electronic copy of the article).*

Yan proposed an 8DOF robot for ultrasound-guided percutaneous prostate intervention therapy [39]. As shown in Fig. (**2**), the ultrasonic probe of the robot has 2DOF, the needle positioning manipulator has 4DOF and a 2DOF driver (needle), and the lifting platform controls the vertical height adjustment of the robot. The ultrasound probe is aligned with the anus by adjusting the posture of the lift platform, which is then attached to the hospital bed. The probe and needle actuators have 2DOF, linear, and rotary, respectively. The needle positioning manipulator uses a parallel mechanism, which slightly improves stiffness. The particle swarm optimization method improves the final puncture accuracy based on the amount of information, and the average needle tip error is between 0.963 mm and 1.846 mm. To improve the accuracy, the system uses the particle swarm optimization method in conjunction with the new mechanical mechanism. The old algorithm is greatly improved compared with other new mechanical mechanisms. However, there are still many drawbacks to ultrasonic guidance, the most serious of which is false negatives. C Hen *et al.* [40] proposed an optimal mechanism for the rapid release of multiple needle insertion into the prostate guided by an ultrasound system. The two driving fingers of the robotic arm realize translation and angle adjustment, and stabilize the soft tissues of the prostate by combining with multi-needle insertion. The duration of the whole experiment is less than 3 minutes, and the average error is less than 0.5 mm. Tang *et al.* [41] proposed to realize prostate puncture surgery by a two-arm robot. One robot arm operated the puncture module and the other operated the ultrasound probe. Combined with the real clockwise tracking algorithm proposed by the author, it can be used for two-dimensional ultrasound in robotic biopsy and BT to achieve high-precision puncture.

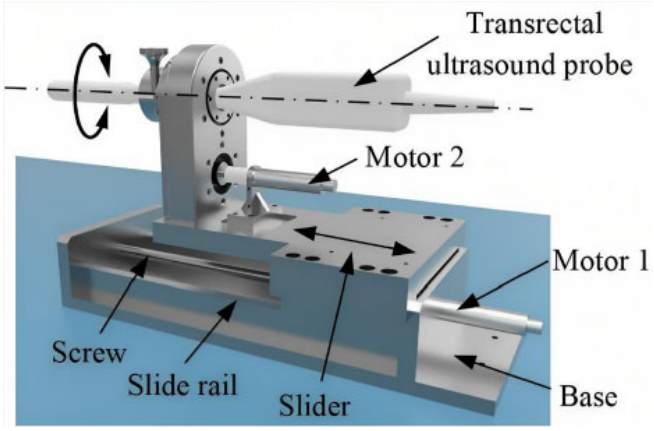

Fig. (2). Prostate intervention robot, proposed by Yan [39]. *(A higher resolution / colour version of this figure is available in the electronic copy of the article).*

2.2. MRI-guided Prostate Intervention Robot

Su *et al.* proposed a piezoelectrically driven prostate puncture robot for MRI-guided prostate puncture therapy [42]. The tensioner in the strap joint is rotated to adjust the distance between the motor shaft of the clamping mech-

anism and the chuck shaft. The linear motor gives the system 2DOF of motion, and the scissor mechanism is used for lifting and lowering [43]. Fischer *et al.* proposed an MRI-guided robot for minimally invasive prostate surgery [16], which includes: a front trapezoidal platform, a back trapezoidal platform, and a needle drive bracket. The trapezoidal platform with 4DOF can be transverse and longitudinal movement and generate angle adjustment. The needle drive bracket is connected to the front trapezoidal platform and back trapezoidal platform through a spherical pair, and the driving mode is suitable for the MRI piezoelectric motor, compared with the pneumatic robot that is more compact. The compact mechanism of the robot and its modular design also make the mechanism more flexible. However, the accumulation of many factors, such as the mechanism and human factors, will lead to a large deviation in the final puncture during the operation. The combination of MRI and US can be tried to plan the path before MRI and transrectal imaging through US during the operation, which will have a good puncture effect. Jiang proposed a 5DOF robot for prostate cancer treatment [44], which is made up of a horizontal pitch, and insert modules connected in series. The cylinders of the horizontal and pitch modules drive the puncture needle adjustment. The insert module is powered by an ultrasonic motor, and the robot is constructed of a polyformaldehyde and copper alloy. Materials and the driving module are chosen for use in an MRI environment. The experimental results show that the tip's error is 0.72 mm. The robot performs high-precision punctures in the MRI environment, avoiding secondary punctures and reducing patient pain. However, the inner diameter of most MRI scanners is about 600mm, which also limits the structure and working angle of the robot and requires a more compact mechanism. Kim *et al.* proposed an MRI-compatible modular needle driver [45]. The device mainly consists of a base robot and a needle driver. The base robot has 4DOF consisting of two trapezoidal connecting rods, and the needle driver has 6+1DOF consisting of a needle gun adapter, a drive package, and two concentric axes in the middle. The 2DOF of rotation is defined as the degrees of freedom of rotation along the axis, and the degrees of freedom of needle drive. The robot drive device is the piezoelectric motor, and the needle drive device is an ultrasonic motor. Dan proposed a 3DOF robot for prostate puncture in the MRI environment [46], which uses a pneumatic drive to adapt to the MRI working environment, and the positioning needle is guided by 2DOF, as shown in Fig. (**3**), where the nut on the rotation axis is used to adjust the length of the needle, and 1DOF is used to achieve linear puncture. The puncture accuracy of the robot was 2.58 mm when tested on animal tissue. Eslami *et al.* proposed a 4DOF MR-compatible parallel robotic system design for transperineal prostate puncture. Most of the robot materials are high-strength polycarbonate (filled with 20% glass), ABS (Acrylonitrile Butadiene Styrene), cast nylon, and other CNC machined materials [47]. The main structure consists of two parallelogram mechanisms (trapezoidal platform) and a slider structure; the different positions of the trapezoidal table allow the needle to form different angles to avoid obstacles. The slider is equipped with a fiber optic limit switch to prevent the slider from colliding with the support (the patient's legs must be open during the operation). A robot for transperineal needle placement is proposed, which is suitable for transperineal prostate biopsy [48-50]. Yiallouras proposed a three-axis robot for prostate treatment based on an MRI environment [51], which mainly realizes linear, rotational, and up and down movement through the rectum.

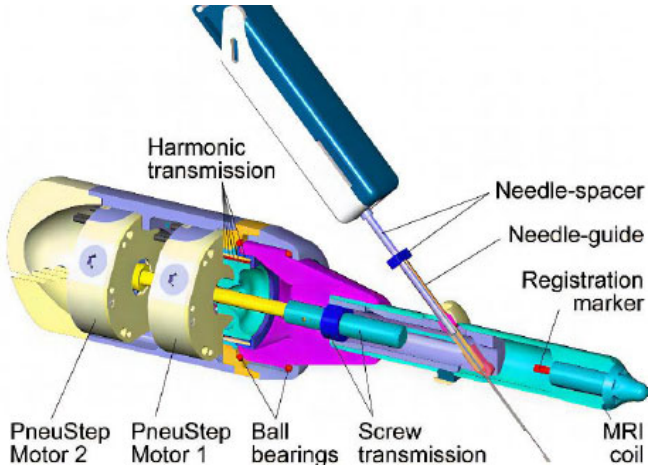

Fig. (3). MRI-guided prostate intervention robot, proposed by Dan [46]. *(A higher resolution / colour version of this figure is available in the electronic copy of the article).*

Patel *et al.* proposed a robot for transperineal prostate biopsy [52]. The robot has 4DOF, with 2DOF translational motion and 2DOF angular motion. Two linear guides are installed on the patient bed plate and fixed by screws so that the whole robot mechanism can generate linear motion through the linear guides. Since it is in the MRI environment, an ultrasonic motor is used to drive the movement of the reference frame by ultrasonic motor. The sterile reference frame is configured in a Z-shape on three orthogonal planes, which is convenient for holding the patient's legs and fixing the skin to be taken out. Through the gelatin puncture experiment under the nuclear magnetic 3T MRI scanner, the obtained data showed that the signal-to-noise ratio was improved by 15.35%, the RMS (Root Mean Square) error of the gelatin surface was 1.5mm, and the maximum error was 2.1 mm. The robot fully utilizes the advantages of MRI combined with medical instruments by ultrasonic motor under MRI conditions. In addition, the robot can not only be easily expanded by individual testing through modular design but can also be used in other aspects of intervention surgery. However, it still has certain limitations in the accumulation of robot mechanism errors and needle deflection errors, and the experiment is based on gelatin tissue. Li *et al.* designed a pneumatic prostate particle implantation robot [53], which includes: an adjustment module that can realize the adjustment of the robot puncture point, needle position, and posture. The function of the module is to realize the puncture of the needle and the implantation of the particle. The modular design idea [54] also makes the mechanism more compact compared with other pneumatic robots. Fig. (**4**) shows 3D

schematic drawings of the execution module and the adjustment mechanism. The implanted cylinder and the breakthrough slide are connected together to drive the puncture cylinder. When the implanted cylinder reaches a certain position, the breakthrough cylinder can quickly achieve puncture. The robot consists of a preformed sliding table, locking cylinder, friction wheel, locking gear, and locking rack. This method of segmental processing solves the difficulty of cylinder position control well. The executive module realizes the movement of the inner needle, outer needle and seed into the inner cavity through three moving sliders. The adjustment is composed of a horizontal moving mechanism and a lifting and pitching mechanism. The horizontal moving mechanism moves in the X and Y directions through the connection of the guide slide block. The lifting and moving mechanism adopts the scissor mechanism to adjust the pitching mechanism of the puncture needle. The cylinder of the robot is made of pure aluminum, which has good heat dissipation and can achieve high-precision positioning in the MRI environment. The trachea joint is made of brass, and the sealing element is made of polyurethane. Due to the pneumatic principle, the puncture speed is extremely fast, so the purpose of high-speed puncture can be realized. Through the experiment, the puncture deviation of the robot is 6.5 mm smaller than the average deviation of the doctor's actual operation. Due to the compressibility of the air, the deviation of the final radioactive particles may be too large. Moreover, the experiment has not been implemented in a real hospital environment, and the experimental data is single. Therefore, the described pneumatic prostate particle implantation robot has certain limitations. Seifabadi *et al.* [55] proposed a 6DOF prostatic intervention robot, including a 4DOF perineal robot and a 2DOF needle steering module, to compensate for errors caused by positioning and organization.

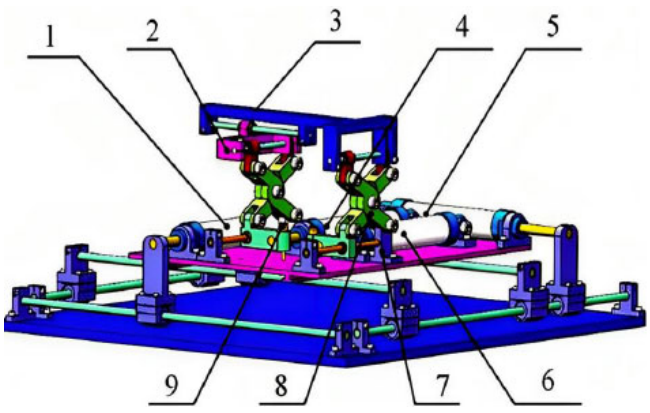

Fig. (4). MRI guided prostate intervention robot, proposed by Li [53]. *(A higher resolution / colour version of this figure is available in the electronic copy of the article).*

CN109124770B describes a prostate puncture robot guided by MRI or CT [56], as shown in Fig. (**5A**), which includes a preloaded detachable probe, a probe fixing frame, a TCP fixed-point control multi-degree of freedom robot with a ranging device, and a computer console. The control can help to complete the operation in the nuclear magnetic environment, which has the advantages of good real-time and high precision compared with the ultrasonic guidance environment. US20150265354 also proposed an MRI-guided prostate puncture robot [57], as shown in Fig. (**5B**). Its driving module can achieve functions including rectal movement and puncture needle deflection, and the driving mode is a pneumatic motor.

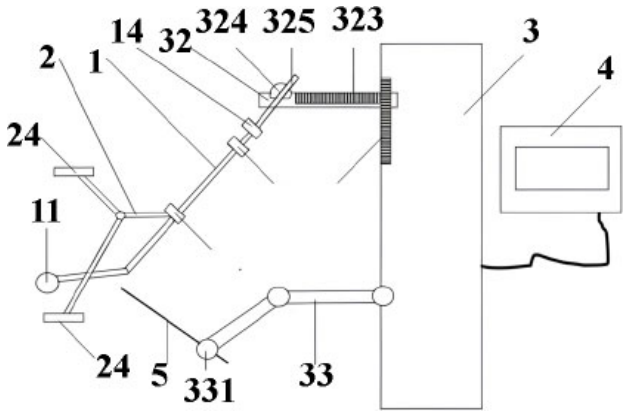

Fig. (5). A. The prostate puncture robot(CN109124770B) [56]. *(A higher resolution / colour version of this figure is available in the electronic copy of the article).*

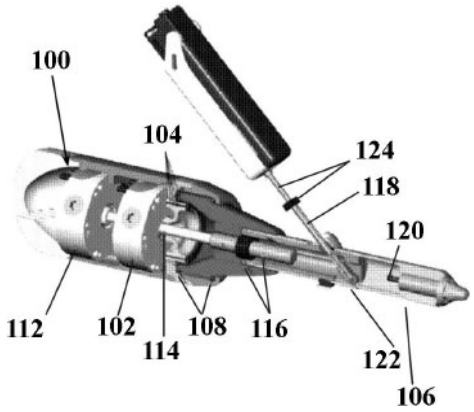

Fig. (5). B. The prostate puncture robot(US20150265354) [57]. MRI-guided prostate intervention robot. *(A higher resolution / colour version of this figure is available in the electronic copy of the article).*

2.3. MRI-US-Guided Prostate Intervention Robot

Prostate cancer is the second most common cancer in men worldwide, which has inspired researchers to develop minimally invasive therapies for localized prostate cancer, such as BT, which is ultrasound-guided, low-cost, radiation-free, and has good real-time performance but poor imaging quality. Although MRI has high imaging quality, MRI is relatively time-consuming and costly. Therefore, Bi *et al.* proposed a US/MRI fusion method with a serial cantilever structure prostate robot [58]. As shown in Fig. (**6A**), the robot adopted an elastic balancing mechanism to achieve the balance of the cantilever beam. The parallelogram linkage mechanism in the robot can reduce the mass and moment of inertia of the cantilever beam, and the deviation of the nee-

dle tip under the experimental environment is less than 2.5 mm. However, at present, bionic materials are used to puncture soft tissues, which will have a large deviation from the actual conditions. The point-based initial registration method is adopted to register US and MRI images, which improves not only the configuration accuracy but also the time. Miah proposed a core-oriented prostate biopsy robot [59], which used the combination of MRI and US to improve image registration and puncture accuracy [60]. The transrectal ultrasound probe was located at one end of the robotic arm. The robot utilized the concept of a double cone, and the increased incidence of puncture surgery performed by the robot could be avoided. Zhang *et al.* [61] proposed a 6DOF prostate radiotherapy robot based on the US-MRI fusion method. The ultrasound probe of the robot is attached to the puncture needle module. A multimodal image deformation registration method based on MCC is proposed to achieve high-precision puncture. However, the registration process of the robot ultrasonic module is complicated, so it is necessary to simplify the registration process without affecting the puncture accuracy in the future. Seifabadi *et al.* [62] proposed a prostatectomy robot guided by MRI-US image fusion. As shown in Fig. (**6B**), the retentor of the ultrasound probe can realize translation and rotation of 2DOF, which can improve the imaging stability of the ultrasound probe. In the future, combined with the corresponding flexible robot, intervention robotic surgery can be realized.

2.4. CT-guided Prostate Intervention Robot

Plitea *et al.* [63] proposed a 5DOF BT robot that does not require a guide plate, but the robot also requires physicians to manually implant radioactive particles, which increases the problem of radiation exposure. As shown in Fig. (**7**), Garg *et al.* [64] improved acubot-rnd7-axis robot by adding rotation and oblique needle insertion. CT scanning was required before the operation, and the robot was fixed on the bed. The total RMS error range of the system obtained by the experiment was between 2.6-4.3 mm. Kim *et al.* [17] proposed a CT-guided 2DOF needle driver (generally combined with the end of the binding robot), a motion mode of translation with ball splines and a set of synchronous gear belts, and rotation adjustment of the needle driver with splines and another set of synchronous gear belts. The maximum error of the final repeatability is 0.16 mm and the standard deviation is 0.0058 mm.

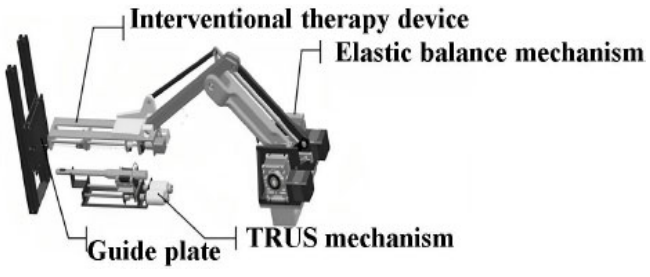

Fig. (6). A. MRI-US guided prostate intervention robot, proposed by Bi [58]. *(A higher resolution / colour version of this figure is available in the electronic copy of the article).*

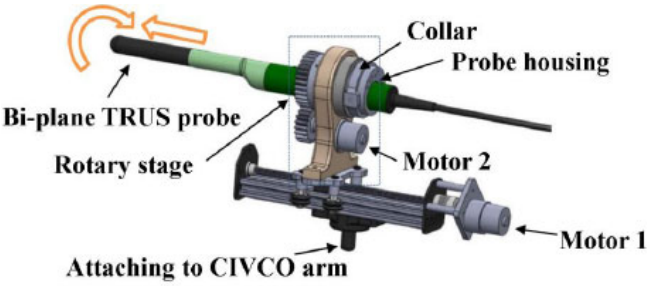

Fig. (6). B. MRI-US guided prostate intervention robot, proposed by Seifabadi [62]. MRI-US guided prostate intervention robot, proposed by (**A**) Bi, (**B**) Seifabadi. *(A higher resolution / colour version of this figure is available in the electronic copy of the article).*

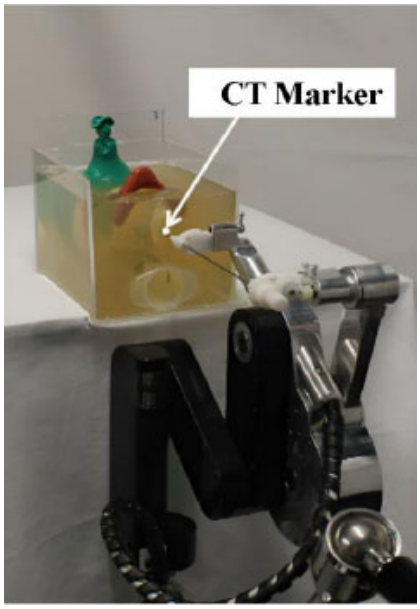

Fig. (7). Guided prostate intervention robots [17]. *(A higher resolution / colour version of this figure is available in the electronic copy of the article).*

3. THE COMPATIBILITY OF PUNCTURE ROBOT AND GUIDED IMAGE SYSTEM AND INTERVENTION TECHNIQUES

Image quality determines the accuracy of intervention surgery. The well-known MRI system often needs to consider the influence of distortion, SNR(Signal-to-Noise Ratio) measurement, and material selection of robot system manufacturing on image quality, and CT-guided robots will also conduct noise analysis. This section mainly discusses the selection of the main manufacturing materials for MRI and CT. The selection of the MRI driver is also discussed.

3.1. Material Selection and Method of Mri Guided Intervention Robots

The material selection for MRI-compatible intervention robots is relatively limited, and ferromagnetic materials, non-conductive materials, and large amounts of metal

Table 1. Ultrasound guided prostate intervention robots.

Published	Author	DOF	Mechanical Structure	Needle Insertion Approach	Research Progress	Human-computer Interaction	Limitation
2012 [21]	Long	7	Two pairs of translation guide, ball screw, rotating mechanism	TP	Robot's median precision is 2.73 mm and 5.46 mm to reach the phantom target	Semi-automatic	The effect of gravity can reduce accuracy
2014 [22]	C. Vaida	5	X, Y, Z 3DOF cantilever, Angle adjustment mechanism	-	-	Fully automatic	Rigidity is poor, flexibility is not high, there are singular points
2014 [23]	Poquet	6	Electromagnetic brake, balance spring and with cable drive	TR	-	Semi-automatic	The presence of a cantilever results in low stiffness (which can be improved by combining a linkage like a parallel quadrilateral)
2018 [15]	Zhang	6	Linear sliding table, linear driving mechanism, rotary driving mechanism, axial vibration mechanism	TR	Improved accuracy by rotating the insertion needle: approximately 87% reduction at 1000rpm at insertion speeds of 20 mm/s.	Fully automatic	The error and other aspects of the cantilever mechanism accumulation will have certain deficiencies
2018 [27]	C	2+3	The puncture adjusting module and the ultrasonic probe adjusting module are connected through a universal joint	TR	-	Fully automatic	The forward solution of parallel robot is complicated and the error between mechanisms will be accumulated
2019 [28]	Ban	2	The inner needle slide table is fixedly connected with the ball screw slide table, and the spring presses the pill and guides the inner needle.	-	Repeatability of the device was within ±0.1 mm	Fully automatic	Poor flexibility, need to rely on high flexibility of the robot
2019 [29]	Lim	4	Poor flexibility, need to rely on high flexibility of the robot	TR	The puncture needle was completed with 1 mm accuracy	semi-automatic	-
2022 [39]	Yan	8	The lifting platform adjusts the height, the needle positioning manipulator is a parallel mechanism, and the needle feeding mechanism	TR	The average error of the tip is between 0.963 mm and 1.846 mm	Fully automatic	Singularity exists and the accuracy needs to be improved
2017 [40]	Chen	4	Vertical slider mechanism, drive unit, guide mechanism, insert mechanism	-	The average error is less than 0.5 mm	Fully automatic	Poor flexibility and inability to avoid important organizations
2019 [41]	Tang	-	Screw slide table as puncture module, ultrasonic probe adjustment module	-	Tip positioning error is 0.6mm, and the minimum tip positioning error is 0.06 mm	Fully automatic	Single plane accuracy is low

Table 2. MRI guided prostate intervention robots.

Published	Author	Dof	Mechanical Structure	Needle Insertion Approach	Research Progress	Human-computer Interaction	Limitation
2012 [43]	Su	6	Synchronous belt, scissors mechanism, pin drive module	TP	RMS has an error of 0.87 mm	Fully automatic	The rigidity is low and the safety needs to be improved
2013 [16]	Fischer	4	The front trapezoidal platform and the back trapezoidal platform are connected with the pin drive bracket through a spherical pair	TP	-	Fully automatic	The accumulation of many factors, such as mechanism and human factors, will lead to a large deviation of final puncture
2014 [44]	Jiang	5	The horizontal module, pitch module and insert module are constituted in series structure	-	The tip of the needle has an error of 0.72 mm	Fully automatic	The structure needs to be more compact
2015 [45]	Kim	4+6+1	Two trapezoidal connecting rods form the base, the biopsy gun adapter, the drive pack, and two concentric shafts in the middle form the concentric shaft	-	-	Fully automatic	General stability, easy to lead to soft tissue movement of the prostate

(Table 2) contd....

Published	Author	Dof	Mechanical Structure	Needle Insertion Approach	Research Progress	Human-computer Interaction	Limitation
2013 [46]	Dan	3	Locate the needle guide. The nut is used to adjust the length of the needle	-	The puncture accuracy was 2.58 mm	Fully automatic	Flexibility is poor, rely on flexibility to get a robot
2016 [47]	Eslami	4	Two parallelogram mechanisms (trapezoidal platform) combined with the slider structure	TP	-	Fully automatic	Poor stiffness
2015 [51]	Yiallouras	3	Linear axis, rotation axis, lifting axis	TR	-	Fully automatic	Simple structure, poor flexibility
2019 [52]	Patel	4	An improved mechanism based on [16]	TP	The RMS error in the gelatin surface is 1.5 mm and the maximum error is 2.1 mm	Fully automatic	The accumulation and experiment of robot mechanism error and needle deflection error are based on gelatin structure, but still have some limitations
2022 [53]	Li	-	Executive module, adjusting module, adjusting module, mechanism joins a locking mechanism, locking mechanism includes: preformed sliding table, locking cylinder, friction wheel, locking gear and locking teeth	-	The puncture deviation of the robot is 6.5 mm smaller than the average deviation of the doctor's actual operation	Fully automatic	The compressibility of air may cause the final radioactive particles to deviate too much
2016 [55]	Seifabadi	6	Adjustment module and steering module	TP	-	Fully automatic	The stiffness is poor and the accuracy is general

Table 3. MRI-US and CT guided prostate intervention robots.

Published	Image Navigation System	Author	DOF	Mechanical Structure	Needle Insertion Approach	Research Progress	Human-computer Interaction	Limitation
2020 [58]	MRI-US	Bi	6	Improved mechanism based on [15]	TR	Tip deviation less than 2.5 mm	Fully automatic	The bionic material used in the experiment will have a large deviation from the actual, and the image registration time is long
2020 [59]	MRI-US	Miah	-	-	TP	-	Fully automatic	-
2016 [61]	MRI-US	Zhang	6	Puncture module and adjustment module	-	-	Fully automatic	The registration process is relatively complicated
2016 [62]	MRI-US	Seifabadi	2	The screw slide provides linear motion and the retainer achieves translation and rotation	-	-	semi-automatic	The stiffness is poor, and the stability needs to be further improved
2015 [63]	CT	Plitea	5	-	-	-	semi-automatic	The stiffness is poor, and the stability needs to be further improved
2017 [17]	CT	Kim	2	The ball splines move linearly with one set of synchronous gear belts, and the splines rotate with another set of synchronous gear belts	-	The total RMS error range of the system is between 2.6-4.3 mm	Fully automatic	The stiffness is poor, and the stability needs to be further improved

should be avoided as much as possible, because the induced eddy current of the scanner will deform the magnetic field, and reducing image artifacts and noise can improve puncture accuracy. General selection: aluminum, brass, titanium, high-strength plastics, and composite materials (nylon, silicone, polyformaldehyde, polypropylene, PTFE, *etc.*) [65-70]. Driving devices are also important in an MRI environment. Currently, the mainstream drivers [71] are: ultrasonic/piezoelectric motor [72-75], pneumatic motor [76-78], hydraulic motor [79-86], and mechanical brake [87, 88]. Piezoelectric/ultrasonic motors and air motors are the most widely used. The main limitations of air motors [89] are precise position control, fine step size, time delay, and nonlinear friction. Future air motors may have better control, smaller size, and as low noise as possible. The posture of the end effector of the robot is extremely important in percutaneous

puncture surgery, so the sensors selected are mostly optical sensors, which will achieve better accuracy in the future, but the price is relatively high.

3.2. Material Selection and Method of CT Guided Intervention Robots

In terms of material selection, MRI-compatible intervention robots are much better than MRI. Generally, glass fiber, carbon-reinforced epoxy resin and ceramics are used. The innomotion robot uses plastic and ceramic materials, and the RCM needle guide robot [90] uses non-ferromagnetic and non-conductive materials. Kim *et al.* [42] proposed a CT-guided 2DOF needle driver using a polymer.

3.3. Image Recognition

To achieve high-precision puncture, not only a flexible mechanism is needed, but also image recognition. Generally, it CT scans the prostate with X-rays, and the images are finally formed based on the principle of different soft tissue densities with different X-ray attenuation levels [91]. However, CT has a low quality for soft tissue imaging and may cause misdiagnosis, so it is generally not used for prostate BT [92].The principle of the ultrasound system is similar to that of CT, which realizes imaging through the different attenuation degrees of different tissues encountered by ultrasound. The final image is represented by gray pixels between black and white of the prostate. The ultrasound system can detect in real-time and obtain the shape, contour and size of the diseased tissue, which has been widely applied to the branching-therapy technology of prostate in the past [93]. Although the ultrasound system has great advantages in a small area, it can sometimes cause false negative phenomena. MRI imaging is mainly performed by attenuation of capacity in different tissues in the environment of a strong magnetic field, and the imaging quality of soft tissues is very high, which can improve the puncture accuracy. However, due to the need to consider the selection of materials under eddy current and magnetic field, artifacts are also easy to be generated [94]. The MRI-US image fusion technology combines the advantages of MRI and US to further improve the puncture accuracy, but the problem of visual prostate soft tissue image registration technology is still a big challenge [95]. It generally includes extrinsic and intrinsic registration methods. At present, the mainstream optimization strategies are simulated annealing algorithm [96, 97], LM (Levenberg-Marquardt) algorithm [98, 99], EM (Expectation Maximization) algorithm [100, 101], and ICP (Iterative Closest Point) algorithm [102-105].

CONCLUSION

This review examines representative prostate intervention robots from the last decade, categorized by different imaging guidelines (US, MRI, MRI-US, and CT), and analyzes their structural design, puncture accuracy, materials, actuators, and compatibility. It is clear that US-guided prostate intervention robotic and MRI systems have received the most attention in the study. However, the US may lead to false negatives and the imaging quality is not as high as MRI, which is expensive and has limitations with respect to the material of the robot. The fusion of MRI and US combines the advantages of real-time imaging and high imaging quality. Therefore, we predict that the US will become the universal image guidance for prostate BT in the near future, and MRI and US fusion-guided prostate intervention robots will become mainstream in the future. Currently, with high-quality image guidance, it is necessary to consider how other means can be used to improve puncture accuracy in order to avoid damage to normal tissue by radioactive particles. Several factors can affect puncture accuracy, such as needle and tissue-induced soft tissue deformation that requires focal displacement prediction, respiratory or physical factors that cause focal displacement, gravity compensation of the robot's master hand, device material compatibility, and drive unit.

CURRENT & FUTURE DEVELOPMENTS

In recent years, the prostate intervention robot has attracted more attention because it can, to some extent, make up for doctors' lack of experience in performing intervention surgery. The physiological shaking of the hand leads to a cheap puncture path and solves the lesion points that cannot be reached by traditional intervention surgery. The structural design and materials of the prostate intervention robot are also great challenges, not only to make the robot more flexible but also to meet the restrictions under different image guidance The most obvious is the MRI-guided intervention robot, where the material must be non-ferromagnetic conductive materials, and drivers are also limited, such as the most common ultrasonic motor and pneumatic motor. In addition, it is believed that the ultrasound probe may cause soft tissue changes during movement in the body, thus shifting the location of focal points, which will lead to deviation from the actual situation in 3D modelling. Therefore, it is also very important to design the ultrasound probe holder for the ultrasound-guided prostate BT robot [106-109]. In this paper, the intervention prostate robot is reviewed and the BT prostate robot is mainly discussed. Based on different image processing techniques, the US, MRI, MRI-US and CT robotic systems and key technologies are discussed. US has the advantages of low price and real-time surgery, but at the same time, the imaging quality is relatively low and may even cause false negative phenomenon. MRI has better soft tissue imaging technology, which can greatly improve puncture accuracy. However, due to its high price, the robotic system must take into account the choice of materials, which results in certain limitations. Although MRI-US fusion imaging technology combines the advantages of US and MRI, the problem of image registration has become the most critical technology. In addition, we found that most robots used US and MRI systems for brachyprostatic surgery, and image fusion technology will become the future trend, while CT image quality is consistent and unsatisfactory, and most of them are applied to intervention surgery in the thoracic and abdominal cavity. Although the image registration technology of MRI-US has high requirements, and there are still great challenges in imaging soft tissue deformation [110],

we boldly predict that MRI-US will gradually become the mainstream image guidance technology of intervention surgical robots in the future.

Tables **1**-**3** show a comparison of the 26 different image-guided prostate intervention robot design options proposed in this paper. All design options were compared in terms of degrees of freedom, experimental accuracy, and with or without automatic mode.

AUTHOR CONTRIBUTIONS

W.Z. and J.Y. contributed to the research design and implementation, as well as the data analysis and manuscript writing.

LIST OF ABBREVIATIONS

BT	=	(BrachyTherapy)
TP	=	(TransPerineal)
TR	=	(TransRectal)
MRI	=	(Magnetic Resonance Imaging)
US	=	(Ultrasound Systems)
CT	=	(Computed Tomography)
RRT	=	(Rapidly-exploring Random Trees)
RCM	=	(Remote Motion Center)
FMC	=	(Free Mode Control)
LMC	=	(Locked Mode Control)
ABS	=	(Acrylonitrile Butadiene Styrene)
RMS	=	(Root Mean Square)
LM	=	(Levenberg-marquardt)
EM	=	(Expectation Maximization)
ICP	=	(Iterative Closest Point)
DOF	=	(Degree-of-freedom)

CONSENT FOR PUBLICATION

Not applicable.

FUNDING

This research was supported by the Opening Project of the Key Laboratory of Advanced Processing Technology and Intelligent Manufacturing (Heilongjiang Province) (No. KFKT202204).

CONFLICT OF INTEREST

The authors declare no conflict of interest, financial or otherwise.

ACKNOWLEDGEMENTS

Declared none.

REFERENCES

[1] O-R. Rocío, L-L. Macarena, S-B. Inmaculada, J-P. Antonio, V-A. Fernando, G-C. Marta, S. María-José, and J-M. José-Juan, "Compliance with the 2018 World Cancer Research Fund/American Institute for Cancer Research cancer prevention recommendations and prostate cancer", *Nutrients,* vol. 12, no. 3, p. 768, 2020. http://dx.doi.org/10.3390/nu12030768 PMID: 32183345

[2] P. Rawla, "Epidemiology of prostate cancer", *World J. Oncol.,* vol. 10, no. 2, pp. 63-89, 2019. http://dx.doi.org/10.14740/wjon1191 PMID: 31068988

[3] C.J.D. Wallis, A. Glaser, J.C. Hu, H. Huland, N. Lawrentschuk, D. Moon, D.G. Murphy, P.L. Nguyen, M.J. Resnick, and R.K. Nam, "Survival and complications following surgery and radiation for localized prostate cancer: An international collaborative review", *Eur. Urol.,* vol. 73, no. 1, pp. 11-20, 2018. http://dx.doi.org/10.1016/j.eururo.2017.05.055 PMID: 28610779

[4] D.L.C. Kee, J. Gal, A.T. Falk, R. Schiappa, M.E. Chand, M. Gautier, J. Doyen, and J.M. Hannoun-levi, "Brachytherapy versus external beam radiotherapy boost for prostate cancer: Systematic review with meta-analysis of randomized trials", *Cancer Treat. Rev.,* vol. 70, pp. 265-271, 2018. http://dx.doi.org/10.1016/j.ctrv.2018.10.004 PMID: 30326422

[5] G. Gandaglia, E. Mazzone, A. Stabile, A. Pellegrino, V. Cucchiara, F. Barletta, S. Scuderi, D. Robesti, R. Leni, A.M. Samanes Gajate, M. Picchio, L. Gianolli, G. Brembilla, F. De Cobelli, M.N. van Oosterom, F.W.B. van Leeuwen, F. Montorsi, and A. Briganti, "Prostate-specific membrane antigen radioguided surgery to detect nodal metastases in primary prostate cancer patients undergoing robot-assisted radical prostatectomy and extended pelvic lymph node dissection: Results of a planned interim analysis of a prospective phase 2 study", *Eur. Urol.,* vol. 82, no. 4, pp. 411-418, 2022. http://dx.doi.org/10.1016/j.eururo.2022.06.002 PMID: 35879127

[6] M. Kim, D. Yoo, J. Pyo, and W. Cho, "Clinicopathological significances of positive surgical resection margin after radical prostatectomy for prostatic cancers: A meta-analysis", *Medicina (Kaunas),* vol. 58, no. 9, p. 1251, 2022. http://dx.doi.org/10.3390/medicina58091251 PMID: 36143928

[7] C. Würnschimmel, M. Wenzel, F. Chierigo, R.S. Flammia, Z. Tian, F. Saad, A. Briganti, S.F. Shariat, N. Suardi, C. Terrone, M. Gallucci, F.K.H. Chun, D. Tilki, M. Graefen, and P.I. Karakiewicz, "External beam radiotherapy and radical prostatectomy are associated with better survival in Asian prostate cancer patients", *Int. J. Urol.,* vol. 29, no. 1, pp. 17-24, 2022. http://dx.doi.org/10.1111/iju.14701 PMID: 34553428

[8] S.S. Dhaliwal, T. Chettibi, S. Wilby, W. Polak, A.L. Palmer, N. Reynaert, and R. Merzouki, "Review of clinical and technological consideration for MRI-guided robotic prostate brachytherapy", *IEEE Trans. Med. Robot. Bionics,* vol. 3, no. 3, pp. 583-605, 2021. http://dx.doi.org/10.1109/TMRB.2021.3097127

[9] A. Sidana, F. Blank, H. Wang, N. Patil, A.K. George, and H. Abbas, "Schema and cancer detection rates for transperineal prostate biopsy templates: A review", *Ther Adv Urol.,* vol. 14, p. 17562872221105019, 2022.

[10] E.J. Bass, A. Pantovic, M.J. Connor, S. Loeb, A.R. Rastinehad, M. Winkler, R. Gabe, and H.U. Ahmed, "Diagnostic accuracy of magnetic resonance imaging targeted biopsy techniques compared to transrectal ultrasound guided biopsy of the prostate: A systematic review and meta-analysis", *Prostate Cancer Prostatic Dis.,* vol. 25, no. 2, pp. 174-179, 2022. http://dx.doi.org/10.1038/s41391-021-00449-7 PMID: 34548624

[11] D.R. Kaye, D. Stoianovici, and M. Han, "Robotic ultrasound and needle guidance for prostate cancer management", *Curr. Opin. Urol.,* vol. 24, no. 1, pp. 75-80, 2014. http://dx.doi.org/10.1097/MOU.0000000000000011 PMID: 24257431

[12] N.P. Gupta, S. Bansal, R. Yadav, R. Khera, K. Ahlawat, D. Gautam, R. Ahlawat, and G. Gautam, "Multiparametric magnetic resonance imaging-transrectal ultrasound fusion prostate biopsy: A prospective, single centre study", *Indian J. Urol.,* vol. 33, no. 2, pp. 134-139, 2017.

http://dx.doi.org/10.4103/0970-1591.203414 PMID: 28469301

[13] A.N. Sridhar, A. Hughes-Hallett, E.K. Mayer, P.J. Pratt, P.J. Edwards, G.Z. Yang, A.W. Darzi, and J.A. Vale, "Image-guided robotic interventions for prostate cancer", *Nat. Rev. Urol.,* vol. 10, no. 8, pp. 452-462, 2013.
http://dx.doi.org/10.1038/nrurol.2013.129 PMID: 23774960

[14] Y. Zhang, Q. Yuan, H. Muhammad Muzzammil, G. Gao, and Y. Xu, "Image-guided prostate biopsy robots: A review", *Math. Biosci. Eng.,* vol. 20, no. 8, pp. 15135-15166, 2023.
http://dx.doi.org/10.3934/mbe.2023678 PMID: 37679175

[15] Y. Liang, D. Xu, B. Wang, Y. Zhang, and Y. Xu, "Experimental study of needle insertion strategies of seed implantation articulated robot", *J. Mech. Med. Biol.,* vol. 18, no. 3, p. 1850023, 2018.
http://dx.doi.org/10.1142/S0219519418500239

[16] S. Eslami, G.S. Fischer, S.E. Song, J. Tokuda, N. Hata, C.M. Tempany, and I. Iordachita, "Towards clinically optimized MRI-guided surgical manipulator for minimally invasive prostate percutaneous interventions: constructive design", *2013 IEEE International Conference on Robotics and Automation,* pp. 1228-1233, 2013.
http://dx.doi.org/10.1109/ICRA.2013.6630728

[17] K.Y. Kim, H.S. Woo, J.H. Cho, and Y.K. Lee, "Development of a two DOF needle driver for CT-guided needle insertion-type interventional robotic system", *2017 26th IEEE International Symposium on Robot and Human Interactive Communication (RO-MAN),* Lisbon, Portugal, 2017, pp. 470-475.
http://dx.doi.org/10.1109/ROMAN.2017.8172344

[18] H. Liang, W. Zuo, D. Kessler, T. Barrett, and Z.T.H. Tse, "A Pneumatic Driven MRI-Guided Robot System for Prostate Interventions", *IEEE Trans. Med. Robot. Bionics,* p. 1, 2024.
http://dx.doi.org/10.1109/TMRB.2024.3389490

[19] W. Jiang, D. Wu, W. Dong, J. Ding, Z. Ye, P. Zeng, and Y. Gao, "Design and validation of a non-parasitic 2R1T parallel hand-held prostate biopsy robot with remote center of motion", *J. Mech. Robot.,* vol. 16, no. 5, p. 051009, 2024.
http://dx.doi.org/10.1115/1.4062793

[20] H. Duan, Y. Zhang, and H. Liu, "Continuous body type prostate biopsy robot for confined space operation", *IEEE Access,* vol. 11, pp. 113667-113677, 2023.
http://dx.doi.org/10.1109/ACCESS.2023.3323312

[21] J.A. Long, N. Hungr, M. Baumann, J.L. Descotes, M. Bolla, J.Y. Giraud, J.J. Rambeaud, and J. Troccaz, "Development of a novel robot for transperineal needle based interventions: focal therapy, brachytherapy and prostate biopsies", *J. Urol.,* vol. 188, no. 4, pp. 1369-1374, 2012.
http://dx.doi.org/10.1016/j.juro.2012.06.003 PMID: 22906671

[22] C. Vaida, N. Plitea, B. Gherman, A. Szilaghyi, B. Galdau, D. Cocorean, F. Covaciu, and D. Pisla, "Structural Analysis and Synthesis of Parallel Robots for Brachytherapy", In: *New Trends in Medical and Service Robots Mechanisms and Machine Science,* vol. 16. Springer: Cham, 2014.
http://dx.doi.org/10.1007/978-3-319-01592-7_14

[23] C. Poquet, P. Mozer, M.A. Vitrani, and G. Morel, "An endorectal ultrasound probe comanipulator with hybrid actuation combining brakes and motors", *IEEE/ASME Trans. Mechatron.,* vol. 20, no. 1, pp. 186-196, 2015.
http://dx.doi.org/10.1109/TMECH.2014.2314859

[24] Y. Zhang, Y. Liang, X. Wang, and Y. Xu, "Design and experimental study of joint torque balance mechanism of seed implantation articulated robot", *Adv. Mech. Eng.,* vol. 7, no. 6, 2015.

[25] I. Khalaji, M. Hadavand, A. Asadian, R.V. Patel, and M.D. Naish, "Analysis of needle-tissue friction during vibration-assisted needle insertion", *2013 IEEE/RSJ International Conference on Intelligent Robots and Systems,* Tokyo, Japan, 2013, pp.4099-4104.
http://dx.doi.org/10.1109/IROS.2013.6696943

[26] A.C. Barnett, M. Feidner, and J.Z. Moore, "Vibration needle tissue cutting with varying tip geometry", *International Manufacturing Science and Engineering Conference, American Society of Mechanical Engineers,* 2015.
http://dx.doi.org/10.1115/MSEC2015-9353

[27] C. Vaida, I. Birlescu, N. Plitea, N. Crisan, and D. Pisla, "Design of a needle insertion module for robotic assisted transperineal prostate biopsy", In: *New Trends in Medical and Service Robots: Design.,* Springer International Publishing, 2018, pp. 1-15.
http://dx.doi.org/10.1007/978-3-319-59972-4_1

[28] G. Ban, C. Li, X. Zhang, G. Liu, Y. Liu, J. Zhao, L. Zhang, and Y. Fan, "Design of A Close-range Radiotherapy Particle Implantation Device", *2019 IEEE International Conference on Robotics and Biomimetics (ROBIO),* Dali, China, 2019, pp.1331-1337.
http://dx.doi.org/10.1109/ROBIO49542.2019.8961469

[29] S. Lim, C. Jun, D. Chang, D. Petrisor, M. Han, and D. Stoianovici, "Robotic transrectal ultrasound guided prostate biopsy", *IEEE Trans. Biomed. Eng.,* vol. 66, no. 9, pp. 2527-2537, 2019.
http://dx.doi.org/10.1109/TBME.2019.2891240 PMID: 30624210

[30] W. Ye, B. Zhang, and Q. Li, "Design of a 1R1T planar mechanism with remote center of motion", *Mechanism Mach. Theory,* vol. 149, p. 103845, 2020.
http://dx.doi.org/10.1016/j.mechmachtheory.2020.103845

[31] J. Li, G. Zhang, A. Müller, and S. Wang, "A family of remote center of motion mechanisms based on intersecting motion planes", *J. Mech. Des.,* vol. 135, no. 9, p. 091009, 2013.
http://dx.doi.org/10.1115/1.4024848

[32] C.H. Kuo, J.S. Dai, and P. Dasgupta, "Kinematic design considerations for minimally invasive surgical robots: an overview", *Int. J. Med. Robot.,* vol. 8, no. 2, pp. 127-145, 2012.
http://dx.doi.org/10.1002/rcs.453 PMID: 22228671

[33] Chunwoo Kim, Doyoung Chang, D. Petrisor, G. Chirikjian, Misop Han, and D. Stoianovici, "Ultrasound probe and needle-guide calibration for robotic ultrasound scanning and needle targeting", *IEEE Trans. Biomed. Eng.,* vol. 60, no. 6, pp. 1728-1734, 2013.
http://dx.doi.org/10.1109/TBME.2013.2241430 PMID: 23358940

[34] W. Wang, B. Pan, Y. Ai, Y. Fu, G. Li, and Y. Liu, "Ultrasound-guide prostate biopsy robot and calibration based on dynamic kinematic error model with POE formula", *Robot. Auton. Syst.,* vol. 166, p. 104465, 2023.
http://dx.doi.org/10.1016/j.robot.2023.104465

[35] Y.L. Fu, and W.R. Wang, *"A transrectal ultrasound image-guided prostatic puncture machine"*, C.N. Patent 114767228 B,

[36] D.Y. Yang, *"An artificial intelligence robot assisted prostate targeted puncture diagnosis and treatment device"*, C.N. Patent 113367777 A, 2021.

[37] H.Z. Zhang, B. Li, G.J. Lin, and Y.P. Lin, *"Prostate biopsy puncture machine guided by ultrasound image"*, C.N. Patent 113331875 B, 2023.

[38] M. Bauman, N. Hungr, A. Leroy, J. Troccaz, and V. Daanen, *"Control system and method for precisely guiding a percutaneous needle toward the prostate"*, U.S. Patent 8702579 B2, 2014.

[39] J. Yan, B. Pan, and Y. Fu, "Ultrasound-guided prostate percutaneous intervention robot system and calibration by informative particle swarm optimization", *Front. Mech. Eng.,* vol. 17, no. 1, p. 3, 2022.
http://dx.doi.org/10.1007/s11465-021-0659-x

[40] S. Chen, B. Gonenc, M. Li, D.Y. Song, E.C. Burdette, I. Iordachita, and P. Kazanzides, "Needle release mechanism enabling multiple insertions with an ultrasound-guided prostate brachytherapy robot", *Annu Int Conf IEEE Eng Med Biol Soc.,* vol. 2017, pp. 4339-4342, 2017.
http://dx.doi.org/10.1109/EMBC.2017.8037816

[41] C. Tang, G. Xie, O.M. Omisore, J. Xiong, and Z. Xia, "A real--time needle tracking algorithm with first-frame linear structure removing in 2D ultrasound-guided prostate therapy", *2019 IEEE International Conference on Robotics and Biomimetics (ROBIO),* Dali, China, 2019, pp. 1240-1245.
http://dx.doi.org/10.1109/ROBIO49542.2019.8961638

[42] L. Chen, T. Paetz, V. Dicken, S. Krass, J.A. Issawi, D. Ojdanić, S. Krass, G. Tigelaar, J. Sabisch, A. Poelgeest, and J. Schaechtele, "Design of a dedicated five degree-of-freedom magnetic resonance imaging compatible robot for image guided prostate biopsy", *J. Med. Device.,* vol. 9, no. 1, p. 015002, 2015.
http://dx.doi.org/10.1115/1.4029506

[43] H. Su, D.C. Cardona, W. Shang, A. Camilo, G.A. Cole, D.C. Rucker, R.J. Webster, and G.S. Fischer, "A MRI-guided concentric tube continuum robot with piezoelectric actuation: a feasibility study", *2012 IEEE International Conference on Robotics and Automation,* Saint Paul, MN, USA, 2012, pp. 1939-1945.
http://dx.doi.org/10.1109/ICRA.2012.6224550

[44] S. Jiang, W. Feng, J. Lou, Z. Yang, J. Liu, and J. Yang, "Mod-

elling and control of a five-degrees-of-freedom pneumatically actuated magnetic resonance-compatible robot", *Int. J. Med. Robot.,* vol. 10, no. 2, pp. 170-179, 2014. http://dx.doi.org/10.1002/rcs.1524 PMID: 23893561

[45] K.Y. Kim, M. Li, B. Gonenc, W. Shang, S. Eslami, and I. Iordachita, "Design of an MRI-compatible modularized needle driver for in-bore MRI-guided prostate interventions", *2015 15th International Conference on Control, Automation and Systems (ICCAS),* 2015. http://dx.doi.org/10.1109/ICCAS.2015.7364595

[46] D. Stoianovici, C. Kim, G. Srimathveeravalli, P. Sebrecht, D. Petrisor, J. Coleman, S.B. Solomon, and H. Hricak, "MRI-safe robot for endorectal prostate biopsy", *IEEE/ASME Trans. Mechatron.,* vol. 19, no. 4, pp. 1289-1299, 2014. http://dx.doi.org/10.1109/TMECH.2013.2279775 PMID: 25378897

[47] S. Eslami, W. Shang, G. Li, N. Patel, G.S. Fischer, J. Tokuda, N. Hata, C.M. Tempany, and I. Iordachita, "In-bore prostate transperineal interventions with an MRI-guided parallel manipulator: system development and preliminary evaluation", *Int. J. Med. Robot.,* vol. 12, no. 2, pp. 199-213, 2016. http://dx.doi.org/10.1002/rcs.1671 PMID: 26111458

[48] A. Patriciu, D. Petrisor, M. Muntener, D. Mazilu, M. Schär, and D. Stoianovici, "Automatic brachytherapy seed placement under MRI guidance", *IEEE Trans. Biomed. Eng.,* vol. 54, no. 8, pp. 1499-1506, 2007. http://dx.doi.org/10.1109/TBME.2007.900816 PMID: 17694871

[49] H. Su, I.I. Iordachita, X. Yan, G.A. Cole, and G.S. Fischer, "Reconfigurable MRI-guided robotic surgical manipulator: prostate brachytherapy and neurosurgery applications", *2011 Annual International Conference of the IEEE Engineering in Medicine and Biology Society (EMBC),* Boston, MA, USA, 2011, pp.2111-2114. http://dx.doi.org/10.1109/IEMBS.2011.6090393

[50] G. Li, H. Su, W. Shang, J. Tokuda, N. Hata, C.M. Tempany, and G.S. Fischer, "A Fully Actuated Robotic Assistant for MRI-Guided Prostate Biopsy and Brachytherapy", *Proc SPIE Int Soc Opt Eng.,* vol. 8671, p. 867117, 2013.

[51] C. Yiallouras, K. Ioannides, T. Dadakova, M. Pavlina, M. Bock, and C. Damianou, "Three-axis MR-conditional robot for high-intensity focused ultrasound for treating prostate diseases transrectally", *J. Ther. Ultrasound,* vol. 3, no. 1, p. 2, 2015. http://dx.doi.org/10.1186/s40349-014-0023-2 PMID: 25657846

[52] N.A. Patel, G. Li, W. Shang, M. Wartenberg, T. Heffter, E.C. Burdette, I. Iordachita, J. Tokuda, N. Hata, C.M. Tempany, and G.S. Fischer, "System integration and preliminary clinical evaluation of a robotic system for MRI-guided transperineal prostate biopsy", *J. Med. Robot. Res.,* vol. 4, no. 2, p. 1950001, 2019. http://dx.doi.org/10.1142/S2424905X19500016 PMID: 31485544

[53] B. Li, L. Yuan, C. Wang, and Y. Guo, "Structural design and analysis of pneumatic prostate seed implantation robot applied in magnetic resonance imaging environment", *Int. J. Med. Robot.,* vol. 18, no. 6, p. e2457, 2022. http://dx.doi.org/10.1002/rcs.2457 PMID: 36063541

[54] Y. Xin, D. Guo, J. Qi, Z. Chen, H. Shao, and G. Yuan, "Prospective clinical study of 125I particle permanent implantation for prostate cancer", *Open Journal of Urology,* vol. 10, no. 3, pp. 52-59, 2020. http://dx.doi.org/10.4236/oju.2020.103007

[55] R. Seifabadi, F. Aalamifar, I. Iordachita, and G. Fichtinger, "Toward teleoperated needle steering under continuous MRI guidance for prostate percutaneous interventions", *Int. J. Med. Robot.,* vol. 12, no. 3, pp. 355-369, 2016. http://dx.doi.org/10.1002/rcs.1692 PMID: 26264564

[56] W. Chen, J.M. Guo, G.M. Wang, Y.F. Yang, and Z.B. Xu, *"A prostate-piercing robot"*, C.N. Patent 109124770 B, 2020.

[57] D. Stoianovici, D. Petrisor, C. Kim, and P. Sebrechts, *"MRI-safe robot for transrectal prostate biopsy"*, U.S. Patent 20150265354, 2015.

[58] J. Bi, and Y. Zhang, "US/MRI guided robotic system for the interventional treatment of prostate", *Int. J. Pattern Recognit. Artif. Intell.,* vol. 34, no. 5, p. 2059014, 2020. http://dx.doi.org/10.1142/S0218001420590144

[59] S. Miah, P. Servian, A. Patel, C. Lovegrove, L. Skelton, T.T. Shah, D. Eldred-Evans, M. Arya, H. Tam, H.U. Ahmed, and M. Winkler, "A prospective analysis of robotic targeted MRI-US fusion prostate biopsy using the centroid targeting approach", *J. Robot. Surg.,* vol. 14, no. 1, pp. 69-74, 2020. http://dx.doi.org/10.1007/s11701-019-00929-y PMID: 30783886

[60] P.R. Martin, D.W. Cool, A. Fenster, and A.D. Ward, "A comparison of prostate tumor targeting strategies using magnetic resonance imaging targeted, transrectal ultrasound-guided fusion biopsy", *Med. Phys.,* vol. 45, no. 3, pp. 1018-1028, 2018. http://dx.doi.org/10.1002/mp.12769 PMID: 29363762

[61] S. Zhang, S. Jiang, Z. Yang, R. Liu, Y. Yang, and H. Liang, "An ultrasound image navigation robotic prostate brachytherapy system based on US to MRI deformable image registration method", *Hell. J. Nucl. Med.,* vol. 19, no. 3, pp. 223-230, 2016. PMID: 27824961

[62] R. Seifabadi, S. Xu, P. Pinto, and B.J. Wood, "A motorized ultrasound system for MRI-ultrasound fusion guided prostatectomy", *Medical Imaging 2016: Image-Guided Procedures, Robotic Interventions and Modeling, SPIE,* vol. 9786, pp. 732-737, 2016.

[63] N. Plitea, A. Szilaghyi, and D. Pisla, "Kinematic analysis of a new 5-DOF modular parallel robot for brachytherapy", *Robot. Comput.-Integr. Manuf.,* vol. 31, pp. 70-80, 2015. http://dx.doi.org/10.1016/j.rcim.2014.07.005

[64] A. Garg, T. Siauw, D. Berenson, J.A.M. Cunha, I.C. Hsu, J. Pouliot, D. Stoianovici, and K. Goldberg, "Robot-guided open-loop insertion of skew-line needle arrangements for high dose rate brachytherapy", *IEEE Trans. Autom. Sci. Eng.,* vol. 10, no. 4, pp. 948-956, 2013. http://dx.doi.org/10.1109/TASE.2013.2276940

[65] H. Elhawary, Z.T.H. Tse, M. Rea, A. Zivanovic, B. Davies, C. Besant, N. de Souza, D. McRobbie, I. Young, and M. Lampérth, "Robotic system for transrectal biopsy of the prostate: real-time guidance under MRI", *IEEE Eng. Med. Biol. Mag.,* vol. 29, no. 2, pp. 78-86, 2010. http://dx.doi.org/10.1109/MEMB.2009.935709 PMID: 20659844

[66] E. Franco, D. Brujic, M. Rea, W.M. Gedroyc, and M. Ristic, "Needle-guiding robot for laser ablation of liver tumors under MRI guidance", *IEEE/ASME Trans. Mechatron.,* vol. 21, no. 2, pp. 931-944, 2016. http://dx.doi.org/10.1109/TMECH.2015.2476556

[67] V. Groenhuis, F.J. Siepel, J. Veltman, and S. Stramigioli, "Design and characterization of Stormram 4: An MRI-compatible robotic system for breast biopsy", *2017 IEEE/RSJ International Conference on Intelligent Robots and Systems (IROS),* Vancouver, BC, Canada, 2017, pp.928-933. http://dx.doi.org/10.1109/IROS.2017.8202256

[68] N.V. Tsekos, E. Christoforou, and A. Ozcan, "A general-purpose MR-compatible robotic system: implementation and image guidance for performing minimally invasive interventions", *IEEE Eng. Med. Biol. Mag.,* vol. 27, no. 3, pp. 51-58, 2008. http://dx.doi.org/10.1109/EMB.2007.910270 PMID: 18519182

[69] S. Jiang, F. Sun, J. Dai, J. Liu, and Z. Yang, "Design and analysis of a tendon-based MRI-compatible surgery robot for transperineal prostate needle placement", *Proc. Inst. Mech. Eng., C J. Mech. Eng. Sci.,* vol. 229, no. 2, pp. 335-348, 2015. http://dx.doi.org/10.1177/0954406214533783

[70] S.T. Kim, Y. Kim, and J. Kim, "Design of an MR-compatible biopsy needle manipulator using pull-pull cable transmission", *Int. J. Precis. Eng. Manuf.,* vol. 17, no. 9, pp. 1129-1137, 2016. http://dx.doi.org/10.1007/s12541-016-0137-2

[71] R. Gassert, A. Yamamoto, D. Chapuis, L. Dovat, H. Bleuler, and E. Burdet, "Actuation methods for applications in MR environments", *Concepts Magn. Reson. Part B Magn. Reson. Eng.,* vol. 29B, no. 4, pp. 191-209, 2006. http://dx.doi.org/10.1002/cmr.b.20070

[72] S. Jiang, J. Lou, Z. Yang, J. Dai, and Y. Yu, "Design, analysis and control of a novel tendon-driven magnetic resonance–guided robotic system for minimally invasive breast surgery", *Proc. Inst. Mech. Eng. H,* vol. 229, no. 9, pp. 652-669, 2015. http://dx.doi.org/10.1177/0954411915599018 PMID: 26334035

[73] T. Zhang, D. Navarro-Alarcon, K.W. Ng, M.K. Chow, Y.H. Liu, and H.L. Chung, "A novel palm-shape breast deformation robot for MRI-guided biopsy", *2016 IEEE International Conference on*

Robotics and Biomimetics (ROBIO), Qingdao, China, 2016, pp.527-532. http://dx.doi.org/10.1109/ROBIO.2016.7866376

[74] D. Navarro-Alarcon, S. Singh, T. Zhang, H.L. Chung, K.W. Ng, M.K. Chow, and Y. Liu, "Developing a compact robotic needle driver for MRI-guided breast biopsy in tight environments", *IEEE Robot. Autom. Lett.,* vol. 2, no. 3, pp. 1648-1655, 2017. http://dx.doi.org/10.1109/LRA.2017.2678542

[75] B. Yang, U.X. Tan, A.B. McMillan, R. Gullapalli, and J.P. Desai, "Design and control of a 1-DOF MRI-compatible pneumatically actuated robot with long transmission lines", *IEEE/ASME Trans. Mechatron.,* vol. 16, no. 6, pp. 1040-1048, 2011. http://dx.doi.org/10.1109/TMECH.2010.2071393 PMID: 22058649

[76] G.S. Fischer, I. Iordachita, C. Csoma, J. Tokuda, S.P. DiMaio, C.M. Tempany, N. Hata, and G. Fichtinger, "MRI-compatible pneumatic robot for transperineal prostate needle placement", *IEEE/ASME Trans. Mechatron.,* vol. 13, no. 3, pp. 295-305, 2008. http://dx.doi.org/10.1109/TMECH.2008.924044 PMID: 21057608

[77] A. Wineland, Y. Chen, and Z. Tsz Ho Tse, "Magnetic resonance imaging compatible pneumatic stepper motor with Geneva drive", *J. Med. Device.,* vol. 10, no. 2, p. 020950, 2016. http://dx.doi.org/10.1115/1.4033244

[78] Y. Wei, Y. Chen, Y. Yang, and Y. Li, "Novel design and 3-D printing of nonassembly controllable pneumatic robots", *IEEE/ASME Trans. Mechatron.,* vol. 21, no. 2, pp. 649-659, 2016. http://dx.doi.org/10.1109/TMECH.2015.2492623

[79] Z. Guo, Z. Dong, K.H. Lee, C.L. Cheung, H.C. Fu, J.D.L. Ho, H. He, W-S. Poon, D.T.M. Chan, and K.W. Kwok, "Compact design of a hydraulic driving robot for intraoperative MRI-guided bilateral stereotactic neurosurgery", *IEEE Robot. Autom. Lett.,* vol. 3, no. 3, pp. 2515-2522, 2018. http://dx.doi.org/10.1109/LRA.2018.2814637

[80] E.D. Williams, M.J. Stebbins, P.R. Cavanagh, D.R. Haynor, B. Chu, M.J. Fassbind, V. Isvilanonda, and W.R. Ledoux, "The design and validation of a magnetic resonance imaging–compatible device for obtaining mechanical properties of plantar soft tissue via gated acquisition", *Proc. Inst. Mech. Eng. H,* vol. 229, no. 10, pp. 732-742, 2015. http://dx.doi.org/10.1177/0954411915606150 PMID: 26405098

[81] B. Jarrahi, R. Gassert, J. Wanek, L. Michels, U. Mehnert, and S.S. Kollias, "Design and application of a new automated fluidic visceral stimulation device for human fMRI studies of interoception", *IEEE J. Transl. Eng. Health Med.,* vol. 4, pp. 1-12, 2016. http://dx.doi.org/10.1109/JTEHM.2016.2538239 PMID: 27551646

[82] E. Mendoza, and J.P. Whitney, "A testbed for haptic and magnetic resonance imaging-guided percutaneous needle biopsy", *IEEE Robot. Autom. Lett.,* vol. 4, no. 4, pp. 3177-3183, 2019. http://dx.doi.org/10.1109/LRA.2019.2925558

[83] Y. Zhang, L. Sun, D. Liang, and H. Du, "Design and workspace analysis of a differential motion rotary style breast interventional robot", *Appl. Bionics Biomech.,* vol. 2020, pp. 1-15, 2020. http://dx.doi.org/10.1155/2020/8852228 PMID: 33488767

[84] Y. Qiu, L. Wu, F. Huang, Z. Huang, Q. Yan, and J. Guo, "MRI--Compatible Hydraulic Drive Needle Insertion Robot", *2021 6th IEEE International Conference on Advanced Robotics and Mechatronics (ICARM),* Chongqing, China, 2021, pp. 86-92. http://dx.doi.org/10.1109/ICARM52023.2021.9536120

[85] S. Frishman, A. Kight, I. Pirozzi, M.C. Coffey, B.L. Daniel, and M.R. Cutkosky, "Enabling in-bore MRI-guided biopsies with force feedback", *IEEE Trans. Haptics,* vol. 13, no. 1, pp. 159-166, 2020. http://dx.doi.org/10.1109/TOH.2020.2967375 PMID: 31976906

[86] J. Dai, Z. He, G. Fang, X. Wang, Y. Li, C.L. Cheung, L. Liang, I. Iordachita, H.C. Chang, and K.W. Kwok, "A robotic platform to navigate MRI-guided focused ultrasound system", *IEEE Robot. Autom. Lett.,* vol. 6, no. 3, pp. 5137-5144, 2021. http://dx.doi.org/10.1109/LRA.2021.3068953

[87] Y. Lin, Y. Shi, F. Wang, J. Zhang, H. Sun, and W. Wu, "Development and placement accuracy evaluation of an MR conditional robot for prostate intervention", *Med. Biol. Eng. Comput.,* vol. 59, no. 5, pp. 1023-1034, 2021. http://dx.doi.org/10.1007/s11517-021-02347-5 PMID: 33860444

[88] M. Lu, Y. Zhang, and H. Du, "Design and control of a novel magnetic resonance imaging-compatible breast intervention robot", *Int. J. Adv. Robot. Syst.,* vol. 17, no. 3, 2020. http://dx.doi.org/10.1177/1729881420927853

[89] A. Melzer, B. Gutmann, T. Remmele, R. Wolf, A. Lukoscheck, M. Bock, H. Bardenheuer, and H. Fischer, "INNOMOTION for percutaneous image-guided interventions: principles and evaluation of this MR- and CT-compatible robotic system", *IEEE Eng. Med. Biol. Mag.,* vol. 27, no. 3, pp. 66-73, 2008. http://dx.doi.org/10.1109/EMB.2007.910274 PMID: 18519184

[90] D. Stoianovici, C. Jun, S. Lim, P. Li, D. Petrisor, S. Fricke, K. Sharma, and K. Cleary, "Multi-imager compatible, MR safe, remote center of motion needle-guide robot", *IEEE Trans. Biomed. Eng.,* vol. 65, no. 1, pp. 165-177, 2018. http://dx.doi.org/10.1109/TBME.2017.2697766 PMID: 28459678

[91] Y. Zhang, B. Li, and L. Yuan, "Study on the control method and optimization experiment of prostate soft tissue puncture", *IEEE Access,* vol. 8, pp. 218621-218643, 2020. http://dx.doi.org/10.1109/ACCESS.2020.3041370

[92] K.K. Yu, and H. Hricak, "Imaging prostate cancer", *Radiol. Clin. North Am.,* vol. 38, no. 1, pp. 59-85, viii, 2000. http://dx.doi.org/10.1016/S0033-8389(05)70150-0 PMID: 10664667

[93] M. Szegedi, C. Boehm, A. Paxton, P. Rassiah-Szegedi, V. Sarkar, H. Zhao, F. Su, K.E. Kokeny, S. Lloyd, J. Tward, and B.J. Salter, "Comparison of transperineal ultrasound image guidance technique to transabdominal technique for prostate radiation therapy", *Med. Phys.,* vol. 47, no. 12, pp. 6113-6121, 2020. http://dx.doi.org/10.1002/mp.14522 PMID: 33020930

[94] L.P. O'Connor, A.H. Lebastchi, R. Horuz, A.R. Rastinehad, M.M. Siddiqui, J. Grummet, C. Kastner, H.U. Ahmed, P.A. Pinto, and B. Turkbey, "Role of multiparametric prostate MRI in the management of prostate cancer", *World J. Urol.,* vol. 39, no. 3, pp. 651-659, 2021. http://dx.doi.org/10.1007/s00345-020-03310-z PMID: 32583039

[95] P. Markelj, D. Tomaževič, B. Likar, and F. Pernuš, "A review of 3D/2D registration methods for image-guided interventions", *Med. Image Anal.,* vol. 16, no. 3, pp. 642-661, 2012. http://dx.doi.org/10.1016/j.media.2010.03.005 PMID: 20452269

[96] N. Makni, I. Toumi, P. Puech, M. Issa, O. Colot, S. Mordon, and N. Betrouni, "A non-rigid registration and deformation algorithm for ultrasound & MR images to guide prostate cancer therapies", *2010 Annual International Conference of the IEEE Engineering in Medicine and Biology,* Buenos Aires, Argentina, 2010, pp.3711-3714. http://dx.doi.org/10.1109/IEMBS.2010.5627656

[97] A. Valsecchi, S. Damas, and J. Santamaria, "Evolutionary intensity-based medical image registration: a review", *Curr. Med. Imaging Rev.,* vol. 9, no. 4, pp. 283-297, 2014. http://dx.doi.org/10.2174/1573405611309660003

[98] M. Carias, *"Comparison of radiofrequency coil configurations for multiple mouse magnetic resonance imaging"*, Doctoral Dissertation, University of Toronto, 2013.

[99] R. Tennakoon, A. Bab-Hadiashar, and Z. Cao, "Nonlinear approaches in three-dimensional medical image registration", In: *Nonlinear Approaches in Engineering Applications: Applied Mechanics Vibration Control, and Numerical Analysis,* 2015, pp. 251-280. http://dx.doi.org/10.1007/978-3-319-09462-5_10

[100] A. Cosse, "Diffeomorphic surface-based registration for MR-US fusion in prostate brachytherapy.Electrotechnical Conference (MELECON)", *2012 16th IEEE Mediterranean, IEEE, Electrotechnical Conference (MELECON),* Mediterranean, 2012, pp. 903-907. http://dx.doi.org/10.1109/MELCON.2012.6196575

[101] Jun Xie, Yifeng Jiang, and Hung-tat Tsui, "Segmentation of kidney from ultrasound images based on texture and shape priors", *IEEE Trans. Med. Imaging,* vol. 24, no. 1, pp. 45-57, 2005. http://dx.doi.org/10.1109/TMI.2004.837792 PMID: 15638185

[102] C. Hennersperger, B. Fuerst, S. Virga, O. Zettinig, B. Frisch, T. Neff, and N. Navab, "Towards MRI-based autonomous robotic US acquisitions: a first feasibility study", *IEEE Trans. Med. Imaging,* vol. 36, no. 2, pp. 538-548, 2017.

http://dx.doi.org/10.1109/TMI.2016.2620723 PMID: 27831861

[103] S.A. Ahmadi, F. Milletari, N. Navab, M. Schuberth, A. Plate, and K. Bötzel, "3D transcranial ultrasound as a novel intra-operative imaging technique for DBS surgery: a feasibility study", *Int. J. CARS,* vol. 10, no. 6, pp. 891-900, 2015.
http://dx.doi.org/10.1007/s11548-015-1191-4 PMID: 25861056

[104] L. Palladino, B. Maris, A. Antonelli, and P. Fiorini, "Autonomy in robotic prostate biopsy through AI-assisted fusion", *2021 20th International Conference on Advanced Robotics (ICAR),* Ljubljana, Slovenia, 2021, pp. 142-147.
http://dx.doi.org/10.1109/ICAR53236.2021.9659396

[105] S. Shakeri, C. Menard, R. Lopes, and S. Kadoury, "Deformable MRI-TRUS surface registration from statistical deformation models of the prostate", *Medical Imaging 2019: Image-Guided Procedures, Robotic Interventions, and Modeling,* vol. 10951, pp. 504-510, 2019.

[106] M.A. Vitrani, M. Baumann, D. Reversat, G. Morel, A. Moreau--Gaudry, and P. Mozer, "Prostate biopsies assisted by comanipulated probe-holder: first in man", *Int. J. CARS,* vol. 11, no. 6, pp. 1153-1161, 2016.
http://dx.doi.org/10.1007/s11548-016-1399-y PMID: 27072834

[107] L. Wang, Y. Zhang, S. Zuo, and Y. Xu, "A review of the research progress of interventional medical equipment and methods for prostate cancer", *Int. J. Med. Robot.,* vol. 17, no. 5, p. e2303, 2021.
http://dx.doi.org/10.1002/rcs.2303 PMID: 34231317

[108] G. Fichtinger, J.P. Fiene, C.W. Kennedy, G. Kronreif, I. Iordachita, D.Y. Song, E.C. Burdette, and P. Kazanzides, "Robotic assistance for ultrasound-guided prostate brachytherapy", *Med. Image Anal.,* vol. 12, no. 5, pp. 535-545, 2008.
http://dx.doi.org/10.1016/j.media.2008.06.002 PMID: 18650122

[109] D.Y. Song, E.C. Burdette, J. Fiene, E. Armour, G. Kronreif, A. Deguet, Z. Zhang, I. Iordachita, G. Fichtinger, and P. Kazanzides, "Robotic needle guide for prostate brachytherapy: Clinical testing of feasibility and performance", *Brachytherapy,* vol. 10, no. 1, pp. 57-63, 2011.
http://dx.doi.org/10.1016/j.brachy.2010.01.003 PMID: 20729152

[110] Y. Zhang, J. Bi, W. Zhang, H. Du, and Y. Xu, "Bi, W. Zhang, H. Du, and Y. Xu, "Recent advances in registration methods for MRI-TRUS fusion image-guided interventions of prostate"", *Recent Pat. Eng.,* vol. 11, no. 2, pp. 115-124, 2017.
http://dx.doi.org/10.2174/1872212110666161201115248